Inhibition of TGF-β and EGF pathway gene expression and migration of oral carcinoma cells by mucosa-associated lymphoid tissue 1

Y Ohyama[1], Y Kawamoto[1], T Chiba[2], G Maeda[2], H Sakashita[1] and K Imai*[,2]

[1]Department of Oral and Maxillofacial Surgery 2, Meikai University, 1-1 Keyakidai, Sakado, Saitama 350-0283, Japan and [2]Department of Biochemistry, School of Life Dentistry at Tokyo, The Nippon Dental University, 1-9-20 Fujimi, Chiyoda-ku, Tokyo 102-8159, Japan

Background: Expression of mucosa-associated lymphoid tissue 1 (MALT1) is inactivated in oral carcinoma patients with worse prognosis. However, the role in carcinoma progression is unknown. Unveiling genes under the control of MALT1 is necessary to understand the pathology of carcinomas.

Methods: Gene data set differentially transcribed in MALT1-stably expressing and -marginally expressing oral carcinoma cells was profiled by the microarray analysis and subjected to the pathway analysis. Migratory abilities of cells in response to MALT1 were determined by wound-healing assay and time-lapse analysis.

Results: Totally, 2933 genes upregulated or downregulated in MALT1-expressing cells were identified. The subsequent pathway analysis implicated the inhibition of epidermal growth factor and transforming growth factor-β signalling gene expression, and highlighted the involvement in the cellular movement. Wound closure was suppressed by wild-type MALT1 (66.4%) and accelerated by dominant-negative MALT1 (218.6%), and the velocities of cell migration were increased 0.2-fold and 3.0-fold by wild-type and dominant-negative MALT1, respectively.

Conclusion: These observations demonstrate that MALT1 represses genes activating the aggressive phenotype of carcinoma cells, and suggest that MALT1 acts as a tumour suppressor and that the loss of expression stimulates oral carcinoma progression.

Squamous cell carcinoma is a most common malignant neoplasm of the oral cavity. The patient prognosis is still worse than that of all cancers combined, and the annual incidence of new cases is predicted to increase in the next few decades (Choi and Myers, 2008; Siegel et al, 2012). Phenotypic alterations of carcinoma cells result from the aberrations of endogenous and exogenous factors, and select aggressive clones to progress carcinomas to the more advanced states. Understanding molecular mechanisms of carcinoma progression and developing the new therapeutic approach are prerequisite for the improvement of prognosis.

Oral carcinoma cells frequently inactivate tumour-suppressive proteins during the disease progression (Choi and Myers, 2008). Our previous study demonstrated that mucosa-associated lymphoid tissue 1 (MALT1) is expressed in the nucleus of oral

epithelial cells (Chiba et al, 2009) and substitutes keratins depending on its expression (Kawamoto et al, 2013). The advanced carcinomas inactivate MALT1 expression by the promoter methylation, and the loss of expression worse the patient prognosis (Chiba et al, 2009). However, nothing is known about the role of loss of expression in the carcinoma progression at present. The MALT1 is made up of three types of domain: a death domain, Ig-like domains, and a caspase-like domain. The B-cell or T-cell receptor antigen signals oligomerise MALT1 with BCL10 and CARMA1/3 into a CBM complex. The MALT1 interacts with BCL10 through its Ig-like domains and induces IκB-kinase catalytic activity, resulting in nuclear factor-κB (NF-κB) activation in lymphocyte lineages (Thome, 2008; McAllister-Lucas et al, 2011). Unveiling gene data sets that are regulated by MALT1

substantiates the role of loss of expression in the carcinoma progression. In this study, we investigated the gene data sets and pathways by microarray analysis and determined the effect on carcinoma cell phenotype by migration assays.

MATERIALS AND METHODS

Cell lines. HSC2 oral carcinoma cells, which marginally express *MALT1*, were obtained from the Cell Resource Center for Biomedical Research Institute of Development, Aging and Cancer (Tohoku University, Sendai, Japan). HSC2 cells stably expressing FLAG-tagged full-length wild-type *MALT1* ($_{wtMALT1}$HSC2 cells) and the NH$_2$ terminal death and Ig-like domains-deleted dominant-negative MALT1 ($_{\Delta MALT1}$HSC2 cells; Che *et al*, 2004) and transfected vector alone ($_{mock}$HSC2 cells) were established previously (Chiba *et al*, 2009). They were maintained in 10% fetal bovine serum and 100 units per ml of penicillin/streptomycin-containing DMEM (Sigma-Aldrich, St. Louis, MO, USA) in a conventional 5% CO$_2$ incubator.

Microarray analysis. Gene-expression profile was measured with RNA extracted from $_{wtMALT1}$HSC2 cells and $_{mock}$HSC2 cells and processed for aRNA synthesis, labelling, and hybridisation by Mitsubishi Chemical Mediscience, Inc. (Tokyo, Japan). First-strand cDNA synthesis with 100 ng of total RNA, synthesis of biotin-labelled aRNA, and clean up were carried out using GeneChip 3′IVT Express Kit (Affymetrix Japan, Tokyo, Japan). For hybridisation, 15 μg of fragmented aRNA was incubated with GeneChip Human Genome U133A 2.0 in 250 μl of hybridisation solution in GeneChip Hybridization Oven 640 (Affymetrix Japan) at 45 °C for 16 h. GeneChips were then washed and stained with GeneChip Fluidics Station 450 (Affymetrix Japan) according to manufacturer's instruction. Microarrays were scanned with GeneChip Scanner 3000 (Affymetrix Japan), and the signals were processed using GeneChip Command Console Software (AGCC, Affymetrix Japan). The scanned images were first assessed by visual inspection, then analysed to generate raw data files saved as CEL files using the default setting of AGCC. Robust Multichip Analysis was used to normalise the different arrays, and further analysis was carried out with GeneSpring GX10 (version 11.5.1, Agilent Technologies, Inc., Tokyo, Japan). Three replicates were used for microarray analysis and statistics. To find differentially expressed genes, we used Aspin-Welch's paired *t*-test and considered the significance when the *P*-value was below 0.05. The Benjamini–Hochberg false discovery rate (FDR) method was used to correct for multiple testing effect. Probe sets were considered to have changed qualitatively in a specific comparison if an adjusted *P*-value of 0.05 was obtained. Their normalised data were used to generate a list of differentially expressed genes between $_{wtMALT1}$HSC2 cells and $_{mock}$HSC2 cells when they had an absolute change of $\geqslant 2$-fold. Gene-expression changes that met these criteria were termed as 'significant RNA state change' and had directional qualities of 'up' or 'down' (i.e., they can be upregulated or downregulated in $_{wtMALT1}$HSC2 cells). The data discussed in this publication have been deposited in NCBI's Gene Expression Omnibus (Edgar *et al*, 2002) and are accessible through GEO Series accession number GSE42335 (http://www.ncbi.nlm.nih.gov/geo/query/acc.cgi?acc=GSE42335).

Functional and pathway analyses of differentially expressed genes. The differentially expressed gene list was ranked according to their fold changes and compared with sets of genes that were annotated according to the gene ontology (GO) for molecular function, cellular component, and biological process (Ashburner *et al*, 2000). Results with *P*-value $\leqslant$ 0.05 and FDR were used identify canonical pathways associated with the differentially expressed genes by uploading the list into the Ingenuity Pathway

Analysis (IPA) website (version 9.0, http://www.ingenuity.com). Briefly, the Ingenuity Knowledge base contains information from scientific publications regarding direct and indirect relationships between genes and proteins. Each identifier was mapped to its corresponding gene object in the Ingenuity knowledge base. These genes, called focus genes, were overlaid onto a global molecular network in the Ingenuity knowledge base. Networks of these focus genes were then algorithmically generated based on the information available in the IPA web site. All of the differentially expressed genes were included in the analysis, and ranked according to *P*-value (Mori *et al*, 2009). In figures represented in this study, the upregulated genes were marked with red and the downregulated genes with green with the intensity of the colour being an indicator of the fold of expression.

Real-time PCR. Total RNA extracted from cell lines was reverse transcribed to cDNA by MultiScribe Reverse Transcriptase (Applied Biosystems, Foster City, CA, USA) and subjected to real-time PCR using the StepOne Real-time PCR system (Applied Biosystems). PCR conditions were 95 °C for 20 s followed by 40 cycles of 95 °C for 1 s and 60 °C for 20 s. The TaqMan probes (Applied Biosystems) specific for *LXN* (Hs00220138_m1), *TFF1* (Hs00907239_m1), *GATA3* (Hs00231122_m1), *TP53* (Hs01034249_m1), *CDH1* (Hs00170423_m1), *FABP4* (Hs01086177_m1), *FABP6* (Hs01031183_m1), *VEGFC* (Hs00153458_m1), *SNAI2* (Hs00950344_m1), *HMGA2* (Hs00171569_m1), *IL6ST* (Hs00174360_m1), *CDH2* (Hs00983062_m1), *PXN* (Hs01104424_m1), and *IL11* (Hs01055413_g1) were used. Expression levels were normalised against *ACTB* (TaqMan Endogenous Control Human *ACTB*, Applied Biosystems). Levels of gene expression ($2^{-\Delta\Delta Ct}$) were determined by the standard curve method (Schmittgen and Livak, 2008).

Immunoblot. Total cell lysates were used for the immunoblot with a standard protocol. The lysates in the SDS sample buffer containing 1 mM phenylmethanesulphonyl fluoride and a protease inhibitor cocktail (Roche Diagnostics GmbH, Mannheim, Germany) were size fractionated by SDS–PAGE gels under reducing conditions and electrotransferred onto PVDF membranes. The membrane was probed with antibodies specific to TFF1, GATA3 (Santa Cruz Biotechnology, Santa Cruz, CA, USA), LXN (R&D Systems, Minneapolis, MN, USA), FABP4, FABP6, or β-actin (Sigma-Aldrich).

Wound-healing and migration assays. Subconfluent cell monolayer (80–90% confluency) with or without *MALT1* short-interfering RNA (siRNA) transfection (50 nM; #18601 siRNA; Ambion, Austin, TX, USA) was maintained in 1% fetal bovine serum-containing culture medium. Silencer Negative Control #1 siRNA (Ambion) was used as a negative control. Wounds were created by the scratch using a pipettman tip and cultured up to 48 h. The wound closure was evaluated by measuring the width of the remaining wound (Sossey-Alaoui *et al*, 2005). The real-time cell electronic sensing assay based on electrical impedance readings in cell monolayers plated in wells containing built-in gold electrodes was performed. We have used the analyzer (xCELLigence RTCA-DP), 16-well e-plates and the integrated software (Roche Diagnostics GmbH). The RTCA System works by measuring the electronic impedance at the cell-sensor electrode interface integrated on the bottom of e-plates (Yu *et al*, 2006). For time-lapse microscopy, $_{wtMALT1}$HSC2 cells, $_{\Delta MALT1}$HSC2 cells, and $_{mock}$HSC2 cells were labelled with CellTracker Green Fluorescent Probe (Lonza, Walkersvill, MD USA) and seed onto 35-mm plastic dishes. After 10 h, the single cell migration was monitored using a laser scanning microscope (LSM 700; Carl Zeiss, Oberkochen, Germany) equipped with a transparent environmental chamber (Climabox, Carl Zeiss) under 5% CO$_2$ in air at 37 °C. The microscope was driven by the IMARIS (Carl Zeiss) every 10 min

during 16 h ($n = 4$). Cell migration was characterised and quantified using an interactive tracking method (Zahm *et al*, 1997).

Statistical analysis. Statistical analyses on the data manipulation for microarray analysis were indicated above. Percentage of wound closure and migration velocities was analysed by Wilcoxon test using JMP 7.0.1 (SAS Institute Inc., Cary, NC, USA).

RESULTS

Genes regulated by MALT1. Genes expressed in $_{wtMALT1}$HSC2 cells and $_{mock}$HSC2 cells were initially compared by the microarray analysis, and 2933 genes with a fold change of $\geqslant \pm 2.0$ and with the $P < 0.05$ were specified (Figure 1A). They included 1433 upregulated and 1500 downregulated genes in $_{wtMALT1}$HSC2 cells. Strict filtering of normalised intensity value with a fold change of $\geqslant \pm 10.0$ (415 probe sets) showed that the upregulated genes ($n = 328$; fold change, 120.5 ± 580.2, mean $\pm$ s.d.) were more robustly changed than the downregulated genes ($n = 87$, 21.2 ± 16.0; $P = 0.002$; Figure 1B). Top 10 for each was shown in Table 1 (complete list was shown in Supplementary Table 1).

Validation of microarray data. Quantitative real-time PCR was done to validate the genes expressed at various levels, and confirmed the expression in an almost same pattern of the microarray analysis (Figure 1C). The differential protein expression encoded by representative genes that suppress (*LXN*, *TFF1*, and *GATA3*) and stimulate (*FABP4* and *FABP6*) carcinoma progression

(Ohmachi *et al*, 2006; Kouros-Mehr *et al*, 2008; Li *et al*, 2011; Nieman *et al*, 2011; Soutto *et al*, 2011) was substantiated at the protein level (Figure 1D). Although expression of other genes was not validated in this study, many of downregulated genes associate with oral carcinoma progression such as *TWIST1*, *LMO4*, *ZEB2*, *WNT3*, and *MMP14* (Shimada *et al*, 2000; Mizunuma *et al*, 2003; Uraguchi *et al*, 2004; Maeda *et al*, 2005; Okamura *et al*, 2009).

GO and pathway analyses. To analyse the function of MALT1-responsive genes, all data sets of genes were first evaluated by the GO analysis. It suggested that the genes are involved in inter- and intra-cellular signalling, cellular organisation, and developmental processes (Table 2). The IPA top three bio-functions were 'Cancer', 'Cellular Movement', and 'Gastrointestinal Disease', and canonical pathways were 'HER2-Signalling in Breast Cancer', 'Glioma Invasiveness Signalling', and 'Role of Tissue Factor in Cancer' (Figure 2). The list with $P < 0.05$ and threshold value of $-\log$ (P-value), 0.05, were summarised in Supplementary Table 2. Other classification of our interests that were not included in the GO analysis but closely correlated with carcinoma progression including extracellular matrix-degrading enzymes, collagens, laminins, integrins, WNT pathways, and cancer and/or epidermal stem cell markers were listed in Supplementary Table 3.

The pathway analysis was performed on all genes identified with an absolute change of $\geqslant 2$-fold. Since the IPA showed a most close association of the gene data sets to 'Cancer', we overviewed 'Molecular Mechanisms of Cancer' to identify the signalling pathway network affected by MALT1. Ras and SMAD pathways occupied central positions in the network (Supplementary
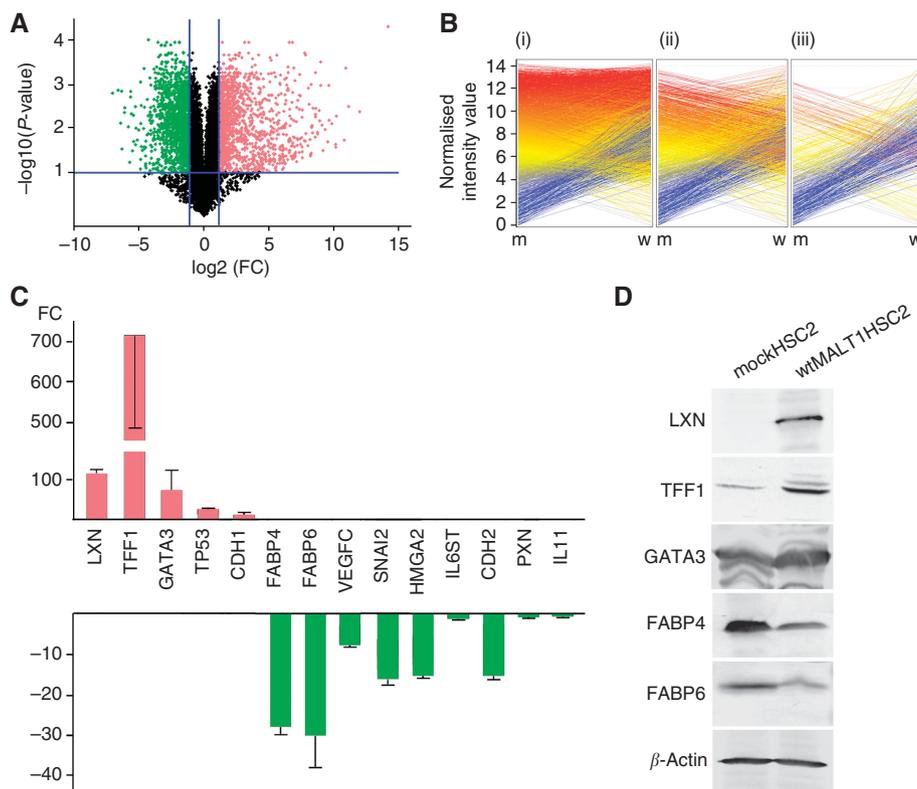
Figure 1. Microarray analysis and its validation by real-time PCR and immunoblot. Log2 fold-change (FC) and their corresponding −log10(*P*-value) of all genes in the microarray were taken for construction of the volcano plot. Genes upregulated and downregulated >2.0-fold change with a *P*-value of <0.05 were depicted in light red and green, respectively. All other genes that were not significantly altered were in black (**A**). Normalised intensity value of gene data set in $_{mock}$HSC2 cells (m) and $_{wtMALT1}$HSC2 cells (w) with different FCs (i, $\geqslant 2.0$; ii, $\geqslant 4.0$; iii, $\geqslant 10.0$) was illustrated. Genes upregulated and downregulated in $_{wtMALT1}$HSC2 cells were depicted in blue and red, respectively (**B**). Expression of genes of interests was analysed by quantitative real-time PCR ($n = 3$). FC of genes of interests in $_{wtMALT1}$HSC2 cells relative to $_{mock}$HSC2 cells were standardised by the expression of *ACTB* (**C**). Protein expression was examined by the immunoblot. β-actin was used as an internal control (**D**).

Table 1. Top 20 genes altered in $_{wtMALT1}$HSC2 cells

Gene symbol	FC	Gene description
Upregulated		
JUP///KRT19	9943.8	Junction plakoglobin///keratin 19
LXN	2407.5	Latexin
TFF1	1377.1	Trefoil factor 1
CXCR4	1196.5	Chemokine (C-X-C motif) receptor 4
SH3YL1	1113.9	SH3 domain containing, Ysc84-like 1
SERPINA3	748.3	Serpin peptidase inhibitor, clade A
TARP///TRBC2	726.8	TCR gamma alternate reading frame protein///T cell receptor gamma constant 2
TBL1X	721.5	Transducin (beta)-like 1X-linked
TARP	597.5	TCR gamma alternate reading frame protein
ATP2A3	523.3	ATPase, Ca + + transporting, ubiquitous
Downregulated		
CYBRD1	97.0	Cytochrome b reductase 1
PSMB8	73.3	Proteasome subunit, beta type, 8
FABP4	64.6	Fatty acid binding protein 4, adipocyte
HOXD10	61.6	Homeobox D10
SERPINB13	60.5	Serpin peptidase inhibitor, clade B, member 13
FABP6	53.4	Fatty acid binding protein 6, ileal
SERPINB2	52.6	Serpin peptidase inhibitor, clade B, member 2
TMPRSS11E///TMPRSS11E2	43.9	Transmembrane protease, serine 11E///transmembrane protease, serine 11E2
PPP4R4	39.2	Protein phosphatase 4, regulatory subunit 4
BCL11A	39.1	B-cell CLL/lymphoma 11A

Abbreviations: CLL = chronic lymphocytic leukemia; FC = fold change; TCR = T-cell receptor.

Table 2. Classification of gene sets by GO analysis

Category	Total gene	Genes/input	*P*-value
Nucleosome	86	43	4.71E − 12
Protein–DNA complex	105	43	3.55E − 5
Chromatin	185	52	2.60E − 6
Basolateral plasma membrane	146	24	1.03E − 5
Protein–DNA complex assembly	112	46	2.79E − 10
Nucleosome assembly	107	46	5.77E − 10
Chromatin assembly	108	46	8.37E − 5
Protein–DNA complex subunit organisation	117	46	1.66E − 9
Nucleosome organisation	114	46	6.78E − 9
DNA packaging	131	46	4.09E − 4
Anatomical structure morphogenesis	811	26	3.77E − 4
Anatomical structure development	1885	56	5.26E − 8
Tissue development	500	31	7.63E − 8
Epidermis development	133	29	2.00E − 4
System development	1565	29	3.23E − 7
Cellular component assembly at cellular level	459	46	4.76E − 7
Cellular component assembly	677	46	4.85E − 7
DNA conformation change	150	46	7.12E − 7
Multicelluar organismal development	2064	162	9.95E − 7
Organ development	1090	29	1.41E − 6
Developmental process	2336	184	1.88E − 6
Chromatin assembly or disassembly	150	49	4.28E − 6
Pathogenesis	21	13	6.91E − 6
Homophilic cell adhesion	114	39	1.19E − 5
Cell–cell adhesion	235		

Abbreviation: GO = gene ontology.

Figure 1). ErbB1 and its ligands (AREG, TGF-α, EREG, and NRG1) and signalling molecules (RAS, PI3K, and PKC) listed in 'ErbB Signalling' were downregulated (Figure 3A). TGF-β pathway genes for TGF-β, TGF-β receptor II, and Smad-2/3/4 (Figure 3B) and many FAK signalling genes, including *ITGs*, *EGFR*, *RHAMM*, *VCL*, *PXN*, and *DOCKs*, were downregulated (Supplementary Figure 2). Although MALT1 is well known to activate NF-κB in lymphocyte lineages (McAllister-Lucas *et al*, 2011), there was no definite predisposition for genes involved in NF-κB activation (Supplementary Figure 3).

Enhanced migration by loss of MALT1 expression. The IPA bio-function analysis suggested a close association of MALT1 in 'Cellular Movement', and enhanced migration is a representative phenomenon of the aggressive behaviours of carcinoma cells (Hanahan and Weinberg, 2011). Therefore, migration of $_{wtMALT1}$HSC2 and $_{\Delta MALT1}$HSC2 cells was compared with that of $_{mock}$HSC2 cells by several sets of experiments. The conventional monolayered wound-healing assay on slide glasses showed 80.5% reduction in wound closure by $_{wtMALT1}$HSC2 cells and the 185.0% enhancement by $_{\Delta MALT1}$HSC2 cells compared with the $_{mock}$HSC2 cells (Figure 4A and B). The siRNA against *MALT1* facilitated the $_{wtMALT1}$HSC2 cell wound closure ($P = 0.003$; Figure 4C; Supplementary Table 4). The $_{\Delta MALT1}$HSC2 cells did not respond to the siRNA because of the lack of binding site in its gene construct. To quantify it more accurately and continuously, the real-time wound-healing assay using the RTCA-DP system was performed. As shown in Figure 4D, the enhanced wound coverage by $_{\Delta MALT1}$HSC2 cells (218.6%) and the reduction by $_{wtMALT1}$HSC2 cells (66.4%) were confirmed. Since the wound closure reflects many aspects of cells (Yilmaz and Christofori, 2010), single cell migration was evaluated by the time-lapse analysis (Figure 4E). Migration velocities of $_{mock}$HSC2 cells were $1.01 \pm 0.05 \, \mu m \, h^{-1}$.

The $_{\Delta MALT1}$HSC2 cells markedly quicken the velocities to $3.06 \pm 0.60 \, \mu m \, h^{-1}$ ($P = 0.021$), and $_{wtMALT1}$HSC2 cells almost unmoved for 16 h ($0.21 \pm 0.01 \, \mu m \, h^{-1}$; $P = 0.021$).

DISCUSSION

A well-established role of NF-κB activation by MALT1 in lymphocytes and enhanced NF-κB activity in advanced oral carcinomas intimate that MALT1 promotes the carcinoma progression (Molinolo *et al*, 2009; McAllister-Lucas *et al*, 2011). However, MALT1 is expressed in normal oral epithelial cells and the loss of expression closely associates with the worse prognosis of carcinoma patients (Chiba *et al*, 2009). Then, we hypothesised that MALT1 has the differential role between epithelial cells and lymphocyte lineages, and analysed gene data sets that were affected by MALT1 in oral carcinoma cells to gain insights into this paradox. Most of the genes registered in 'NF-κB Signalling' in the IPA pathway database were unaffected or downregulated by MALT1, and the upregulated were limited to three genes (data not shown) among the 54 NF-κB-induced genes in head and neck carcinoma cells that were previously reported (Chung *et al*, 2006).
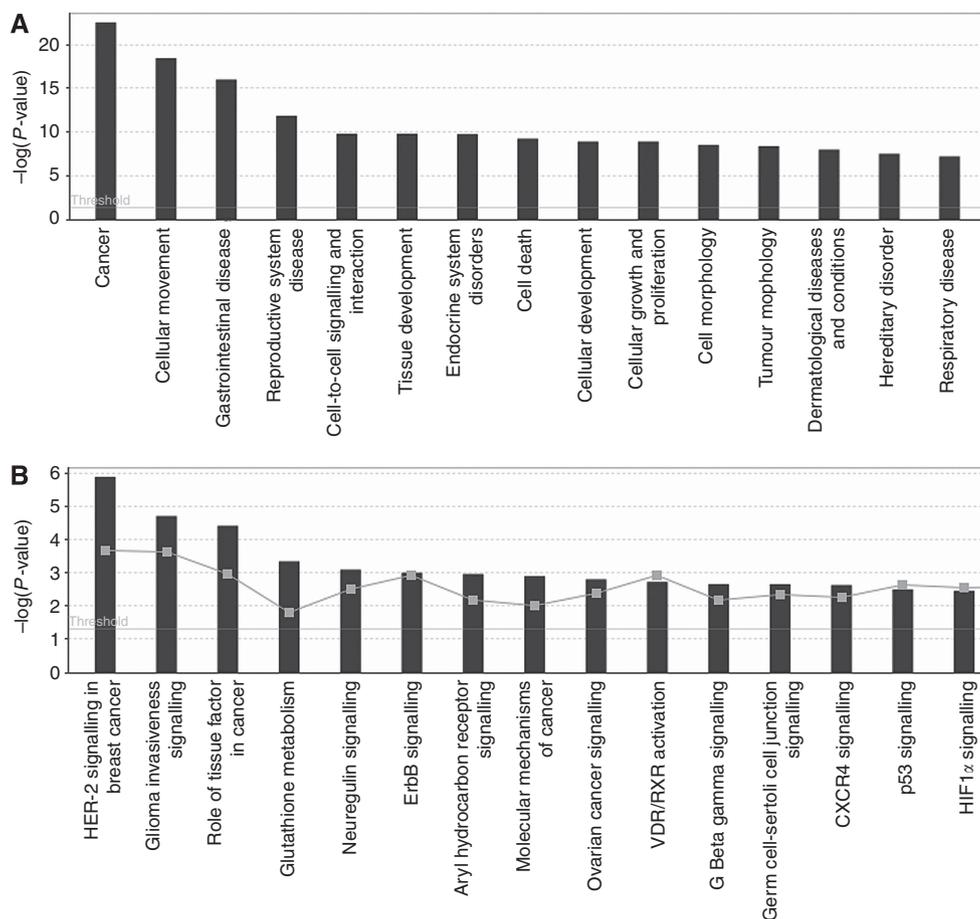
Figure 2. Ingenuity pathway analysis of the genes. The significance of each function or canonical pathway was determined based on the *P*-value by right-tailed Fisher's exact test and with threshold <0.05. The top 15 possible bio-functions (**A**) and canonical pathways (**B**) of genes regulated by MALT1 were shown. Ratio of number of genes in a given pathway satisfying the cutoff and total number of genes present in those pathways was determined by the pathway analysis.

Comparative analysis using IPA demonstrated that the genes downregulated by MALT1 affect EGF and TGF-β pathways and cellular movement, suggesting the stimulation of oral carcinoma aggressiveness by loss of MALT1 expression.

EGFR encoding EGFR (ErbB1, HER-1), a most predominant EGF receptor in head and neck carcinomas (Bei *et al*, 2004), was downregulated. Although other EGF receptors (ErbB2–4) were upregulated, their expression and pathological role in head and neck carcinomas are a controversial issue (Schoppmann *et al*, 2010; Bussu *et al*, 2012; Zanaruddin *et al*, 2013). The EGFR ligands, *AREG*, *TGFA*, and *EREG* downregulated by MALT1, are over-expressed in oral carcinomas and stimulate proliferation of carcinoma cells (Rubin Grandis *et al*, 1996; Tsai *et al*, 2006; Shigeishi *et al*, 2008). Mucosa-associated lymphoid tissue 1 also downregulated EGF signalling molecules, RAS (*HRAS* and *NRAS*) and PKC (*PKCA*, *PKCI*, and *PKCQ*). The amplification of *EGFR* loci *per se* attributes to oral carcinoma development and progression (Sheu *et al*, 2009), and EGFR-mediated pathway is strongly activated in an aggressive subset of oral carcinoma with worse prognosis (Ang *et al*, 2002). Although the frequency of *EGFR* active mutation in oral carcinomas is controversial (Hsieh *et al*, 2011; Mclntyre *et al*, 2012), MALT1 may negatively regulate the pathway by the suppression of gene expression regardless of the presence or absence of mutation. These data suggest the liberation of EGF-EGFR pathway from the suppression upon loss of MALT1 expression.

In parallel with the suppressive role for EGF signalling gene expression, MALT1 downregulated *TGFB2*, *TGFBR*, *SMAD2*, *SMAD3*, and *SMAD4*. A protein complex made of these SMADs is crucial for the TGF-β-TGFBR2 signal transduction (Roberts and Wakefield, 2003). Although TGF-β acts as a potent tumour suppressor at the early stage of carcinoma progression, it stimulates cell proliferation, invasion, metastasis, and angiogenesis at the late stage (Roberts and Wakefield, 2003). Loss of MALT1 expression occurs at the late stage of oral carcinoma progression (Chiba *et al*, 2009). Mucosa-associated lymphoid tissue 1 also downregulated genes encoding gp130 (*IL6ST*) and IL-11 (*IL11*), which stimulate carcinoma progression under the TGF-β pathway (Calon *et al*, 2012). These data imply that the loss of expression facilitates oral carcinomas to activate TGF-β signalling and pathway at the late stage of progression.

Since EGF and TGF-β signalling frequently interact each other and co-regulate gene expression that enhance aggressive phenotypes of carcinoma cells (Kretzschamar *et al*, 1997; Wendt *et al*, 2010; Deharvengt *et al*, 2012), it is difficult to discern which signalling has a principal effect on the target gene expression in $_{wtMALT1}$HSC2 cells. Of note, a mesenchyme-specific transcriptional factor, *HMGA2*, that is upregulated by these signalling induces epithelial–mesenchymal transition (EMT) in carcinoma cells (Li *et al*, 1997; Thuault *et al*, 2006). Induction of the EMT gains carcinomas invasive and chemo-resistant properties (Yilmaz and Christofori, 2010; Hanahan and Weinberg, 2011). HMGA2 is predominantly expressed at invasive front oral carcinoma cells showing the EMT and in the patients with worse prognosis (Miyazawa *et al*, 2004), and MALT1 expression rapidly declines at the invasive front carcinoma cells (Chiba *et al*, 2009). HMGA2 represses *CDH1* expression through *SNAI2*, *ZEB2*,
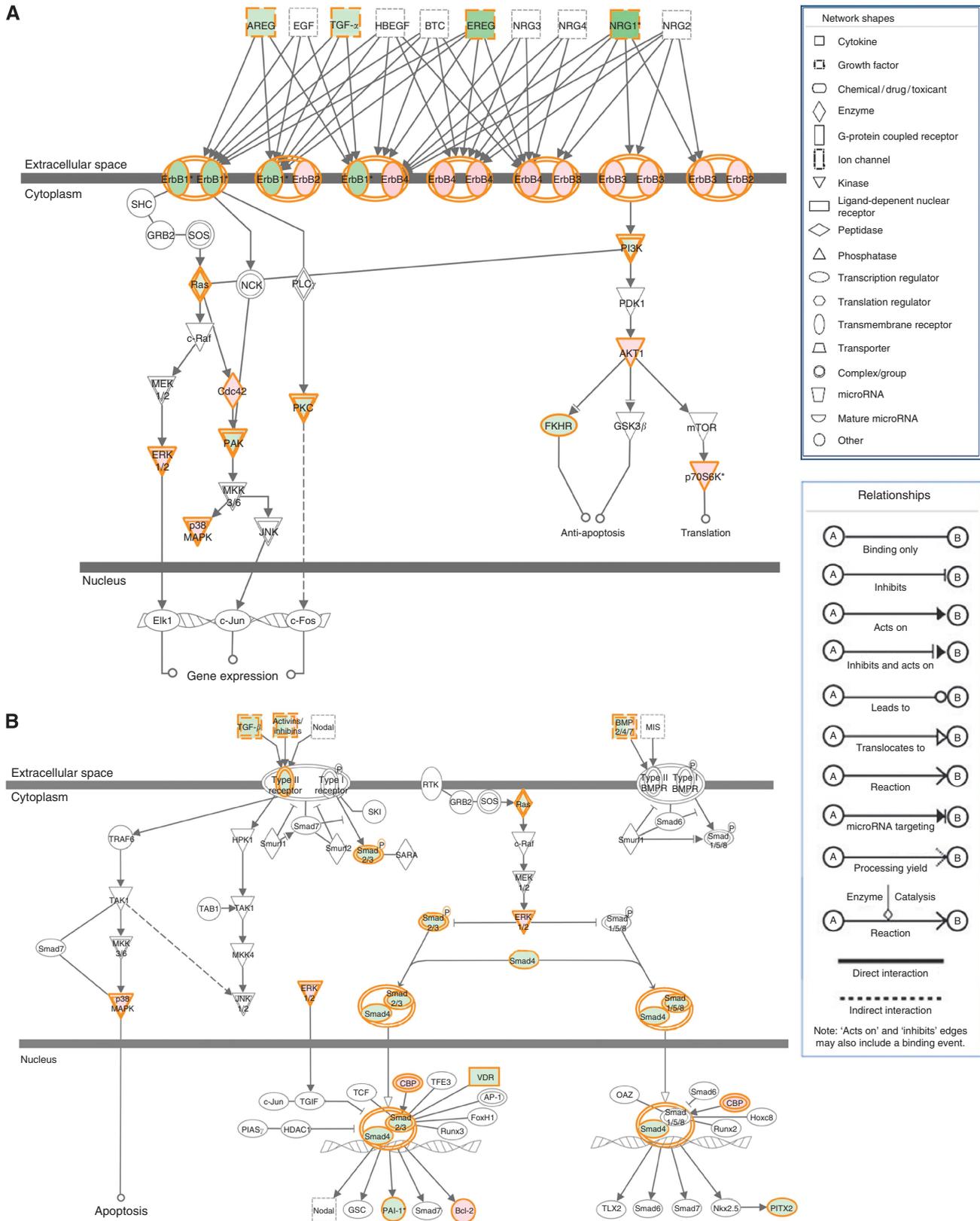
Figure 3. 'ErbB signalling' and 'TGF-β pathway' in the canonical pathway. Functional interacting network among gene data sets was uploaded in the Ingenuity Pathway Analysis tool and the network of 'ErbB Signalling (**A**)' and 'TGF-β pathway (**B**)'. Genes from our data set and falling in this network were shown in either red (upregulated) or green (downregulated).

and *TWIST1* (Li *et al*, 1997; Thuault *et al*, 2008), which were downregulated in wtMALT1HSC2 cells. As numbers of previous studies established a fact that inactivation of E-cadherin (*CDH1*) expression is a critical determinant for aggressive carcinomas (Hanahan and

Weinberg, 2011; Hashimoto *et al*, 2012), expression status of MALT1 may have a great impact on oral carcinoma progression.

Mucosa-associated lymphoid tissue 1 also suppressed other EMT inducers (WNT3, FGFs, PDGFs, IL6R, and FGFRs) and
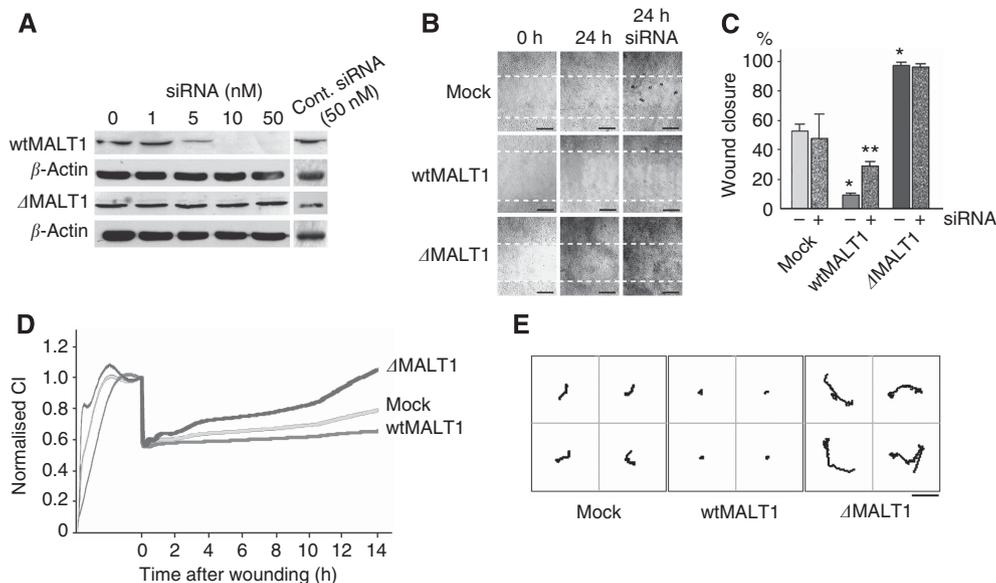
Figure 4. Migration of carcinoma cells. (A) Knock-down of MALT1 protein expression in $_{wtMALT1}$HSC2 cells and $_{\Delta MALT1}$HSC2 cells by the siRNA against *wtMALT1*. The protein expression was probed by the immunoblotting using an anti-FLAG antibody. **(B)** Migration of cells 24 h after injury in the presence or absence of 50 nM *MALT1* siRNA. White broken lines represent the original wound edges. Scale bar = 1 mm. **(C)** Percentage of wound closure at 24 h. The graph indicates means ± s.d. of wound closure at 24 h ($n = 5$). *$P < 0.001$ (compared with mock + siRNA) and **$P < 0.005$ (compared with wtMALT1 without siRNA). **(D)** Real-time sensing wound-healing assay. The coverage of wounds was monitored by the xCELLigence system until 14 h after injury. **(E)** Representative examples of $_{wtMALT1}$HSC2 (wtMALT1), $_{\Delta MALT1}$HSC2 (ΔMALT1), and $_{mock}$HSC2 (mock) cell migration for 16 h using time-lapse microscopy ($n = 4$). Scale bar = 50 µm.

related genes encoding FAK signalling (integrins and paxillin), extracellular matrix-degrading enzymes (MMPs, ADAMs, plasminogen activators, kallikreins and cathepsins), CD44, SPARC, collagens, laminins, Jagged2, and podoplanin (Supplementary Table 1). It appears likely that loss of MALT1 expression activate the EMT machinery.

Enhanced migration is one of most representative characteristics of the EMT (Yilmaz and Christofori, 2010; Hanahan and Weinberg, 2011). Strong suppression of the migration by MALT1 supports our hypothesis that MALT1 has a distinct role in oral carcinoma cells from lymphoma cells. Since TGF-β and EGF pathways synergistically accelerate the EMT and migration of carcinoma cells, their liberation from the suppression by MALT1 may have a key readout circuitry in oral carcinoma progression. Detailed analysis for the role of MALT1 on the pathways should contribute to understand the pathology of oral carcinomas and to develop novel therapeutic strategies for the carcinoma patients.

REFERENCES

Ang KK, Berkey BA, Tu X, Zhang HZ, Katz R, Hammond EH, Fu KK, Milas L (2002) Impact of epidermal growth factor receptor expression on survival and pattern of relapse in patients with advanced head and neck carcinoma. *Cancer Res* **62**: 7350–7356.

Ashburner M, Ball C, Blake J, Botstein D, Butler H, Cherry M, Tarver L, Kasarskis A, Lewis S, Matese JC, Richardson JE, Ringwald M, Rubin GM,

Sherlock G (2000) Gene ontology: tool for the unification of biology. *Nat Genet* **25**: 25–29.

Bei R, Budillon A, Masuelli L, Cereda V, Vitolo D, Di Gennaro E, Ripavecchia V, Palumbo C, Ionna F, Losito S, Modesti A, Kraus MH, Muraro R (2004) Frequent overexpression of multiple ErbB receptors by head and neck squamous cell carcinoma contrast with rare antibody immunity in patients. *J Pathol* **204**: 317–325.

Bussu F, Ranelletti FO, Gessi M, Graziani C, Lanza L, Paludetti G, Almadori G (2012) Immunohistochemical expression patterns of the HER4 receptors in normal mucosa and in laryngeal squamous cell carcinomas: antioncogenic significance of the HER4 protein in laryngeal squamous cell carcinoma. *Laryngoscope* **122**: 1724–1733.

Calon A, Espinet E, Paloma-Pnnce S, Tauriello DVF, Iglesias M, Céspedes MV, Sevillano M, Nadal C, Jung P, Zhang XHF, Byrom D, Riera A, Rossel D, Mangues R, Massagué J, Sancho E, Batlle E (2012) Dependency of colorectal cancer on a TGF-β-driven program in stromal cells of metastasis initiation. *Cancer Cell* **22**: 571–584.

Che T, You Y, Wang D, Tanner MJ, Dixit VM, Lin X (2004) MALT1/paracaspase is a signaling component down-stream of CARMA1 and mediates T cell receptor-induced NF-κB activation. *J Biol Chem* **279**: 15870–15876.

Chiba T, Maeda G, Kawashiri S, Kato K, Imai K (2009) Epigenetic loss of mucosa-associated lymphoid tissue 1 expression in patients with oral carcinomas. *Cancer Res* **69**: 7216–7223.

Choi S, Myers JN (2008) Molecular pathogenesis of oral squamous cell carcinoma: implications for therapy. *J Dent Res* **87**: 14–32.

Chung CH, Parker JS, Ely K, Carter J, Yi Y, Murphy BA, Ang KK, El-Nagger AK, Zanation AM, Cmelak AJ, Levy S, Slebos RJ, Yarbrough WG (2006) Gene expression profiles identify epithelial-mesenchymal transition and activation of nuclear factor-κB signaling as characteristic of high-risk head and neck squamous cell carcinoma. *Cancer Res* **66**: 8210–8218.

Deharvengt S, Marmarelis M, Korc M (2012) Concomitant targeting of EGF receptor, TGF-beta and SRC points to a novel therapeutic approach in pancreatic cancer. *PLoS One* **7**: e39684.

Edgar R, Domrachev M, Lash AE (2002) Gene Expression Omnibus: NCBI gene expression and hybridization array data repository. *Nucleic Acids Res* **30**: 207–210.

Hanahan D, Weinberg RA (2011) Hallmarks of cancer: the next generation. *Cell* **144**: 646–674.

Hashimoto T, Soeno Y, Maeda G, Taya Y, Aoba T, Nasu M, Kawashiri S, Imai K (2012) Progression of oral squamous cell carcinoma accompanied

with reduced E-cadherin expression but not cadherin switch. *PLoS One* 7: e47899.

Hsieh CH, Chang JW, Hsieh JJ, Hsu T, Huang SF, Liao CT, Wang HM (2011) Epidermal growth factor mutations in patients with oral cavity cancer in a betel nut chewing-prevalent area. *Head Neck* 33: 1758–1764.

Kawamoto Y, Ohyama Y, Chiba T, Yagishita H, Sakashita H, Imai K (2013) Proteomic identification of keratin alterations with enhanced proliferation of oral carcinoma cells by loss of mucosa-associated lymphoid tissue 1 expression. *Int J Oncol* (in press).

Kouros-Mehr H, Kim JW, Bechis SK, Werb Z (2008) GATA-3 links tumor differentiation and dissemination in a luminal breast cancer model. *Cancer Cell* 13: 141–152.

Kretzschamar M, Doody J, Massagué J (1997) Opposing BMP and EGF signaling pathways converge on the TGF-beta family mediator Smad1. *Nature* 389: 618–622.

Li D, Lin HH, McMahon M, Ma H, Ann DK (1997) Oncogenic raf-1 induces the expression of non-histone chromosomal architectural protein HMGI-C via a p44/p42 mitogen-activated protein kinase-dependent pathway in salivary epithelial cells. *J Biol Chem* 272: 25062–25070.

Li Y, Basang Z, Ding H, Lu Z, Ning T, Wei H, Cai H, Ke Y (2011) Latexin expression is downregulated in human gastric carcinomas and exhibits tumor suppressor potential. *BMC Cancer* 11: 121.

Maeda G, Chiba T, Okazaki M, Satoh T, Taya Y, Aoba T, Kato K, Kawashiri S, Imai K (2005) Expression of SIP1 in oral squamous cell carcinomas: implications for E-cadherin expression and tumor progression. *Int J Oncol* 27: 1535–1541.

McAllister-Lucas LM, Baens M, Lucas PC (2011) MALT1 protease: a new therapeutic target in B lymphoma. *Clin Cancer Res* 17: 6623–6631.

Mclntyre JB, Bose P, Klimowicz AC, Brockton NT, Petrillo S, Matthews W, Easaw J, Magliocco A, Dort JC (2012) Specific and sensitive hydrolysis probe-based real-time PCR detection of epidermal growth factor receptor variant III in oral squamous cell carcinoma. *PLoS One* 7: e31723.

Miyazawa J, Mitoro A, Kawashiri S, Chada KK, Imai K (2004) Expression of mesenchyme-specific gene HMGA2 in squamous cell carcinomas of the oral cavity. *Cancer Res* 64: 2024–2029.

Mizunuma H, Miyazawa J, Sanada K, Imai K (2003) The LIM-only protein, LMO4, and the LIM domain-binding protein, LDB1, expression in squamous cell carcinomas of the oral cavity. *Br J Cancer* 88: 1543–1548.

Molinolo AA, Amornphimoltham P, Squarize CH, Castilho RM, Patel V, Gutkind JS (2009) Dysregulated molecular networks in head and neck carcinogenesis. *Oral Oncol* 45: 324–334.

Mori R, Xiong S, Wang Q, Tarabolous C, Shimada H, Panteris E, Danenberg KD, Danenberg PV, Pinski JK (2009) Gene profiling and pathway analysis of neuroendocrine transdifferentiated prostate cancer cells. *Prostate* 69: 12–23.

Nieman KM, Kenny HA, Penicka CV, Ladanyi A, Buell-Gutbrod Z, Zillhardt MR, Romero IL, Carey MS, Mills GB, Hotamisligil GS, Yamada SD, Peter ME, Gwin K, Lengyel E (2011) Adipocytes promote ovarian cancer metastasis and provide energy for rapid tumor growth. *Nat Med* 17: 1498–1503.

Ohmachi T, Inoue H, Mimori K, Tanaka F, Sasaki A, Kanda T, Fujii H, Yanaga K, Mori M (2006) Fatty acid binding protein 6 is overexpressed in colorectal cancer. *Clin Cancer Res* 12: 5090–5095.

Okamura H, Yoshida K, Haneji T (2009) Negative regulation of TIMP1 is mediated by transcription factor TWIST1. *Int J Oncol* 35: 181–186.

Roberts AB, Wakefield LM (2003) The two facets of transforming growth factor β in carcinogenesis. *Proc Natl Acad Sci USA* 100: 8621–8623.

Rubin Grandis J, Melhem MF, Barnes EL, Tweardy DJ (1996) Quantitative immunohistochemical analysis of transforming growth factor-alpha and epidermal growth factor receptor in patients with squamous cell carcinoma of the head and neck. *Cancer* 78: 1284–1292.

Schmittgen DD, Livak KJ (2008) Analyzing real-time PCR data by the comparative C_T method. *Nat Protoc* 6: 1101–1108.

Schoppmann SF, Jesch B, Friedrich J, Wrba F, Schultheis A, Pluschnig U, Maresch J, Hejna M, Birner P (2010) Expression of Her-2 in carcinomas of the esophagus. *Am J Surg Pathol* 34: 1868–1873.

Sheu JJ, Hua CH, Wan L, Yj Lin, Lai MT, Tseng HC, Jinawath N, Tsai MF, Chang NW, Lin CF, Lin CC, Hsieh LJ, Wang TL, IeM Shih, Tsai FJ (2009)

Functional genomic analysis identified epidermal growth factor receptor activation as the most common genetic event in oral squamous cell carcinoma. *Cancer Res* 69: 2568–2576.

Shigeishi H, Higashikawa K, Hiraoka M, Fujimoto S, Mitani Y, Ohta K, Takeichi M, Kamata N (2008) Expression of epiregulin, a novel epidermal growth factor ligand associated with prognosis in human oral squamous cell carcinomas. *Oncol Rep* 19: 1557–1564.

Shimada T, Nakamura H, Yamashita K, Kawata R, Murakami Y, Fujimoto N, Sato H, Seiki M, Okada Y (2000) Enhanced production and activation of progelatinase A mediated by membrane-type 1 matrix metalloproteinase in human oral squamous cell carcinomas: implications for lymph node metastasis. *Clin Exp Metastasis* 18: 179–188.

Siegel R, Naishadham D, Jemal A (2012) Cancer statistics, 2012. *CA Cancer J Clin* 62: 10–29.

Sossey-Alaoui K, Li X, Ranalli TA, Cowell JK (2005) WAVE3-mediated cell migration and lamellipodia formation are regulated downstream of phosphatidylinositol 3-kinase. *J Biol Chem* 280: 21748–21755.

Soutto M, Belkhiri A, Piazuelo MB, Schneider BG, Peng D, Jiang A, Washington MK, Kokoye Y, Crowe SE, Zaika A, Correa A, Peek Jr RM, El-Rifai W (2011) Loss of TFF1 is associated with activation of NF-kB-mediated inflammation and gastric neoplasia in mice and human. *J Clin Invest* 121: 1753–1767.

Takayama S, Hatori M, Kurihara Y, Kinugasa Y, Shirota T, Shintani S (2009) Inhibition of TGF-beta1 suppresses motility and invasiveness of oral squamous cell carcinoma cell lines via modulation of integrins and down-regulation of matrix-metalloproteinases. *Oncol Rep* 21: 205–210.

Thome M (2008) Multifunctional roles of MALT1 in T-cell activation. *Nat Rev Immunol* 8: 495–500.

Thuault S, Tan EJ, Peinado H, Cano A, Heldin CH, Moustakas A (2008) HMGA2 and Smads co-regulate SNAIL1 expression during induction of epithelial-to-mesenchymal transition. *J Biol Chem* 283: 33437–33446.

Thuault S, Valcourt U, Petersen M, Manfioletti G, Heldin CH, Moustakas A (2006) Transforming growth factor-beta employs HMGA2 to elicit epithelial-mesenchymal transition. *J Cell Biol* 174: 175–183.

Tsai ST, Yang KY, Jin YT, Lin YC, Chang MT, Wu LW (2006) Amphiregulin as a tumor promoter for oral squamous cell carcinoma: involvement of cyclooxygenase 2. *Oral Oncol* 42: 381–390.

Uraguchi M, Morikawa M, Shirakawa M, Sanada K, Imai K (2004) Activation of WNT family expression and signaling in squamous cell carcinomas of the oral cavity. *J Dent Res* 83: 327–332.

Wendt MK, Smith JA, Schiemann WP (2010) Transforming growth factor-β-induced epithelial-mesenchymal transition facilitates epidermal growth factor-dependent breast cancer progression. *Oncogene* 29: 6485–6498.

Yamada T, Tsuda M, Ohba Y, Kawaguchi H, Totsuka Y, Shindoh M (2008) PTHrP promotes malignancy of human oral cancer cell downstream of the EGFR signaling. *Biochem Biophys Res Commun* 368: 575–581.

Yilmaz M, Christofori G (2010) Mechanism of motility in metastasizing cells. *Mol Cancer Res* 8: 629–642.

Yu N, Atienza JM, Bernard J, Blanc S, Zhu J, Wang X, Xu X, Abassi YA (2006) Real-time monitoring of morphological changes in living cells by electronic cell sensor arrays: an approach to study G protein-coupled receptors. *Anal Chem* 78: 35–43.

Zahm JM, Kaplan H, Hérard AL, Doriot F, Pierrot D, Somelette P, Puchelle E (1997) Cell migration and proliferation during the in vitro wound repair of the respiratory epithelium. *Cell Motil Cytoskeleton* 37: 33–43.

Zanaruddin SN, Saleh A, Yang YH, Hamid S, Mustafa WM, Khairul Bariah AA, Zain RB, Lau SH, Cheong SC (2013) Four-protein signature accurately predicts lymph node metastasis and survival in oral squamous cell carcinoma. *Hum Pathol* 44: 417–426.

Supplementary Information accompanies this paper on British Journal of Cancer website (http://www.nature.com/bjc)